

Revisiting Slider-Pusher Systems as Flat Systems: Model-Based Insights for Contact-Rich Manipulation

Sander De Witte, Tom Lefebvre, and Guillaume Crevecoeur

Abstract—This paper revisits the planar slider-pusher system, a classic illustration of contact-rich manipulation, from the perspective of differential flatness. Under quasi-static assumptions, we derive a general kinematic model that holds for arbitrary planar slider shapes and circular pusher geometries. We show that this system exhibits differential flatness, enabling direct trajectory planning and controller synthesis using the center of mass as a flat output. Leveraging this property, we propose two control strategies for trajectory tracking: a cascaded quasi-static feedback strategy and a dynamic feedback linearization approach. We validate these strategies through closed-loop simulations incorporating perturbed models and input noise, as well as experimental results using a physical setup with a finger-like pusher and vision-based state detection. The real-world experiments confirm the applicability of the simulation gains, highlighting the practicality and robustness of the proposed methods and the model’s utility in real-world robotic manipulation tasks.

I. INTRODUCTION

Recent advances in robotic manipulation balance between model-based control and increasingly data-driven learning approaches. This paper revisits the planar slider-pusher system as a minimal, yet rich, example for contact-rich manipulation, highlighting its differential flatness property and the performance of a simplified model-based approach. Flatness enables system trajectories to be described through a lower-dimensional flat output, simplifying planning and feedback control.

Slider-pusher dynamics have been extensively studied, from early foundational work [1], [2], [3] to more recent data-driven approaches [4], [5], [6]. Many models adopt the quasi-static assumption, where inertial effects are negligible compared to friction [7], [8], [9], [10]. Under this simplification, a differential kinematic model relates pusher input velocity to the slider’s planar motion — though prior studies focus mainly on rectangular sliders.

Even with these assumptions, the system remains hybrid and under-actuated [7], often requiring computationally intensive planning and model-predictive control. To address this, we introduce an additional assumption: negligible friction at the pusher contact point relative to support forces. This yields a compact quasi-static model applicable to arbitrary slider shapes with circular pushers. Based on this model, we identify conditions for differential flatness, a structural property of nonlinear systems [11], [12] that simplifies control synthesis.

All authors are with the Dynamic Design Lab (D²LAB), Department of Electromechanical, Systems and Metal Engineering, Ghent University, Belgium. Correspondence: sander.dewitte@ugent.be



Fig. 1: Overlay of snapshots from one of the cameras, showing dynamic feedback linearization in action on the setup. The reference trajectory is shown in blue, while the executed path is yellow.

Exploiting this flatness, we develop two closed-loop position tracking controllers for rectangular sliders. The first is an ad-hoc cascaded feedback approach; the second applies dynamic feedback linearization, which is feasible since flat systems are also feedback-linearizable [13], [14], [15]. Both strategies focus on position tracking and are validated in simulation under model perturbations and noise, as well as in real-world experiments as seen in Fig. 1.

II. SYSTEM MODEL

We model a planar slider-pusher system with arbitrary, smooth slider geometries and a spherical pusher, as seen in Fig. 2. The system state is given by $\mathbf{x} = (x \ y \ \theta \ \phi)^\top$, where x and y denote the Cartesian coordinates of the slider in the global frame of reference, θ denotes the slider’s planar orientation and ϕ thus determines the contact point. Further, we assume that the velocity of the pusher, expressed in the global frame of reference, can be controlled. Thus we can

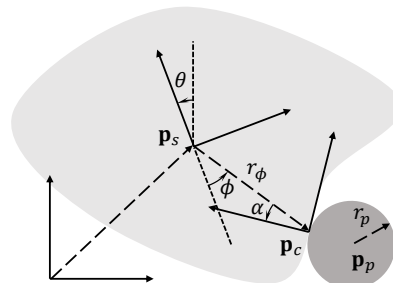


Fig. 2: Geometry of the slider-pusher system.

define an input variable, $\mathbf{u} \in \mathbb{R}^2$, as $\mathbf{u} = (u_x \ u_y)^\top$, where u_x and u_y denote the global velocity of the pusher. The smooth slider shape is described by a function $r(\phi)$, which defines the distance from the center of the pusher to the contact point as a function of the contact angle ϕ . The pusher radius is denoted by r_p , and we assume that the pusher is always in contact with the slider.

Two key assumptions simplify the dynamics:

- Inertial forces are negligible (quasi-static limit surface model).
- Friction at the contact point is negligible compared to the slider-ground interaction.

The relation between contact geometry and motion leads to a compact, reduced model after expressing \mathbf{u} in a rotated local frame:

$$\begin{aligned} \mathbf{u} &= \mathbf{R}(\theta)\tilde{\mathbf{u}}, \\ \tilde{\mathbf{u}} &= \mathbf{R}(\phi)\tilde{\tilde{\mathbf{u}}}, \\ \tilde{\tilde{\mathbf{u}}} &= \mathbf{R}(\alpha)\tilde{\tilde{\tilde{\mathbf{u}}}}, \end{aligned} \quad (1)$$

The derivation is omitted for brevity, but the final equations governing the system dynamics are:

$$\begin{aligned} \dot{x} &= -P(\phi) \sin(\theta + \phi + \alpha) \tilde{\tilde{\tilde{u}}}_y, \\ \dot{y} &= P(\phi) \cos(\theta + \phi + \alpha) \tilde{\tilde{\tilde{u}}}_y, \\ \dot{\theta} &= \Theta(\phi) \tilde{\tilde{\tilde{u}}}_y, \\ \dot{\phi} &= \Phi_x(\phi) \tilde{\tilde{\tilde{u}}}_x + \Phi_y(\phi) \tilde{\tilde{\tilde{u}}}_y, \end{aligned} \quad (2)$$

where

$$\begin{aligned} P(\phi) &= \frac{\beta^2 r(\phi)^2 + \beta^2 r'(\phi)^2}{\beta^2 r(\phi)^2 + \beta^2 r'(\phi)^2 + r(\phi)^2 r'(\phi)^2}, \\ \Theta(\phi) &= \frac{r(\phi) r'(\phi) \sqrt{r(\phi)^2 + r'(\phi)^2}}{\beta^2 r(\phi)^2 + \beta^2 r'(\phi)^2 + r(\phi)^2 r'(\phi)^2}, \\ \Phi_x(\phi) &= \frac{1}{\sqrt{r(\phi)^2 + r'(\phi)^2} + r_p(1 + f(\phi))}, \\ \Phi_y(\phi) &= -\Phi_x(\phi) \frac{r'(\phi) r(\phi) (r(\phi)^2 + r_p \sqrt{r(\phi)^2 + r'(\phi)^2})}{\beta^2 r(\phi)^2 + \beta^2 r'(\phi)^2 + r(\phi)^2 r'(\phi)^2}. \end{aligned} \quad (3)$$

The parameter β describes the slider's resistance to rotational motion relative to translation, reflecting how easily the object spins under external forces. The angle α accounts for the local orientation of the slider's surface normal at the contact point and is determined entirely by the geometry via

$$\tan(\alpha) = -\frac{r'(\phi)}{r(\phi)}. \quad (4)$$

For a rectangular slider, with a geometry characterized by a width $2a$ and a height $2b$, one can further verify that $\alpha = -\phi$. It follows that $\tilde{\tilde{\mathbf{u}}} = \tilde{\mathbf{u}}$. The circumference itself is parametrized as follows:

$$\begin{aligned} r(\phi) &= b \frac{1}{\cos(\phi)}, \\ r'(\phi) &= b \frac{\tan(\phi)}{\cos(\phi)}. \end{aligned} \quad (5)$$

Substitution of these conditions into the model (2) yields:

$$\begin{aligned} \dot{x} &= -\frac{\beta^2}{\beta^2 + b^2 \tan(\phi)^2} \sin(\theta) \tilde{u}_y, \\ \dot{y} &= \frac{\beta^2}{\beta^2 + b^2 \tan(\phi)^2} \cos(\theta) \tilde{u}_y, \\ \dot{\theta} &= \frac{b \tan(\phi)}{\beta^2 + b^2 \tan(\phi)^2} \tilde{u}_y, \\ \dot{\phi} &= \frac{\cos(\phi)^2}{b} \tilde{u}_x - \frac{\cos(\phi)^2}{b} (b + r_p) \frac{b \tan(\phi)}{\beta^2 + b^2 \tan(\phi)^2} \tilde{u}_y. \end{aligned} \quad (6)$$

We can compare this model with earlier work where the contact point was described using its distance, d , relative to the symmetry axis of the slider [16]. It follows that

$$\begin{aligned} d &= b \tan(\phi), \\ \dot{d} &= b \frac{1}{\cos(\phi)^2} \dot{\phi}. \end{aligned} \quad (7)$$

One then easily verifies that the following alternative model representation can be retrieved, as documented earlier:

$$\dot{d} = \tilde{u}_x - (b + r_p) \frac{d}{\beta^2 + d^2} \tilde{u}_y. \quad (8)$$

In conclusion, for uniform pressure distributions we have that

$$\beta^2 = \frac{1}{3} \sqrt{a^2 + b^2}. \quad (9)$$

III. DIFFERENTIAL FLATNESS ANALYSIS

Differential flatness is a powerful property of certain nonlinear systems that allows all state and input variables to be expressed as functions of a so-called flat output and its derivatives [12], [11]. If such a flat output exists, system trajectories can be freely designed without solving differential equations, making flatness a useful tool for planning and control.

For the quasi-static slider-pusher system, we explore whether flat coordinates exist — starting with the slider's centre of mass as a candidate. Manipulating the system equations reveals that flatness can only be achieved if the slider's boundary $r(\phi)$ satisfies a specific geometric condition:

$$r^2 + 2(r')^2 - r''r = 0. \quad (10)$$

This equation characterizes a family of shapes for which the slider-pusher system is flat with respect to its centre of mass. Notably, it implies a fixed relationship between the slider's contact geometry and the flatness property. Once this condition is satisfied, the remaining states and inputs — including the slider's orientation θ , contact angle ϕ , and the inputs \tilde{u}_x , \tilde{u}_y — can be fully reconstructed from the flat output (position) and its derivatives. This flatness result naturally extends to any static point on the slider. If the centre of mass is a flat output, any fixed offset point on the slider also qualifies, since its position is simply a rigid transformation of the centre of mass.

Solving the geometric condition yields the explicit form:

$$r(\phi) = A \frac{1}{\cos(\phi - B)}, \quad (11)$$

which corresponds to polygonal sliders, such as rectangles, when applied piecewise. Each face of a polygon satisfies this relation, and the complete shape is stitched together across its edges. This highlights that flatness is a general property for polygonal slider-pusher systems.

After some algebraic manipulation, we can derive the following flat expressions:

$$\begin{aligned}\theta &= -\arctan\left(\frac{\dot{x}}{\dot{y}}\right) + B_i, \\ \phi &= \arctan\left(\frac{\beta^2 \frac{\dot{x}\ddot{y} - \ddot{x}\dot{y}}{\sqrt{\dot{x}^2 + \dot{y}^2}^3}}{A_i}\right) - B_i, \\ \tilde{u}_x &= (A_i + r_p) \frac{\dot{x}\ddot{y} - \ddot{x}\dot{y}}{\dot{x}^2 + \dot{y}^2} + \beta^2 \frac{\dot{x}\ddot{y} - \ddot{x}\dot{y}}{\sqrt{\dot{x}^2 + \dot{y}^2}^3} \\ &\quad + 3\beta^2 \frac{(\dot{x}\ddot{y} - \ddot{x}\dot{y})(\dot{x}\ddot{x} + \dot{y}\ddot{y})}{\sqrt{\dot{x}^2 + \dot{y}^2}^5}, \\ \tilde{u}_y &= \left(1 + \beta^2 \frac{(\dot{x}\ddot{y} - \ddot{x}\dot{y})^2}{(\dot{x}^2 + \dot{y}^2)^3}\right) \sqrt{\dot{x}^2 + \dot{y}^2}.\end{aligned}\quad (12)$$

For rectangular sliders, we limit our discussion to the bottom face. The other faces are simply permutations of this solution. In this case, we have $B = 0$ and $A = b$. If we use the relative distance to parameterize the contact point rather than the contact angle, the flat expression becomes

$$d = \beta^2 \frac{\dot{x}\ddot{y} - \ddot{x}\dot{y}}{\sqrt{\dot{x}^2 + \dot{y}^2}^3}. \quad (13)$$

IV. CONTROL STRATEGIES

As mentioned before, flatness is a useful property for control synthesis. It is particularly advantageous to solve path planning problems, and is used abundantly in tracking control [17], [18], [19], [20], [16], [21], [22], [23], [24], [25], [26], [27], [28], [29]. Flatness-based trajectory optimization applied to slider pusher was investigated by [16], [30], [31].

This section discusses two closed-loop tracking strategies tailored specifically to flat slider-pusher systems. First, we will discuss an ad-hoc cascaded (quasi-)static feedback strategy. Second, since the system that we will address is flat, and therefore proven to be dynamic feedback linearizable [13], [14], [15], we also develop such a strategy.

Given the developments in the previous sections, we can work with the following rectangular slider model. Note that we can write this model in general state-space form

$$\dot{\xi} = \mathbf{f}(\xi) + \mathbf{g}(\xi)v, \quad (14)$$

with state $\xi = (x, y, \theta, d)$, and input $v = (\tilde{u}_x, \tilde{u}_y)$.

The slider-pusher system is under-actuated. Therefore we will only pursue tracking of a desired position signal, given by x_d and y_d . The position signal may be static or dynamic. In the latter case, we also assume to have access to every time derivative of the desired position signal. Every control strategy assumes access to a measurement of the slider-pusher state, ξ . Two control strategies are proposed based on the flatness property:

1) Quasi-Static Feedback Control: The first control strategy is a cascaded ad-hoc approach that decomposes the tracking problem into nested subgoals, each stabilized on a different time scale. Because the slider cannot align position, orientation, and offset simultaneously with only two control inputs, the controller sequentially enforces these objectives: first driving the slider toward the desired position, then adjusting its orientation, and finally steering the pusher offset. Each stage applies an exponential error decay law to generate reference signals for the next loop, ensuring stability and smooth convergence.

At the outer loop, reference velocities \dot{x}_r and \dot{y}_r are computed based on position errors. These are then used to derive a reference orientation θ_r and normal velocity $\tilde{u}_{y,r}$. The desired angular velocity $\dot{\theta}_r$ follows from θ_r , which leads to calculating a target offset d_r . Finally, the offset velocity \dot{d}_r and the tangential input $\tilde{u}_{x,r}$ are determined, completing the cascade. This structure can be enhanced by replacing first-order error decay with second-order dynamics, using gain parameters tuned to reflect decreasing time constants through the cascade.

2) Dynamic Feedback Linearization: Our second control strategy exploits the fact that any differentially flat system is also dynamic feedback linearizable [14]. This enables the design of linear controllers in a transformed extended state-space.

Definition 1 (Dynamic feedback linearization [32]):

A system is dynamic feedback linearizable if there exist auxiliary states $\gamma \in \mathbb{R}^{n_\gamma}$ and dynamic feedback of the form

$$\begin{aligned}\dot{\gamma} &= \mathbf{a}(\xi, \gamma) + \mathbf{b}(\xi, \gamma)v, \\ v &= \alpha(\xi, \gamma) + \beta(\xi, \gamma)v,\end{aligned}$$

with an extended transformation $\chi = \eta(\xi, \gamma)$ such that the extended system becomes fully linearizable: $\dot{\chi} = \mathbf{A}\chi + \mathbf{B}v$.

Designing a tracking controller then reduces to choosing v to stabilize the linear system, and applying the inverse transformation to compute the control input v for the original nonlinear system. A simple stabilizing choice is linear state feedback:

$$v = v_d + \mathbf{K}(\chi_d - \chi). \quad (15)$$

For our system, the flatness implies $\chi = (x, y, \dot{x}, \dot{y}, \ddot{x}, \ddot{y})$ and $v = (\ddot{x}, \ddot{y})$. Since $\xi \in \mathbb{R}^4$ and $\chi \in \mathbb{R}^6$, the auxiliary state must satisfy $\gamma \in \mathbb{R}^2$. Two practical choices for γ are:

a) Choice 1.: Define γ_1 as the translational speed magnitude and γ_2 as the angle of the acceleration vector:

$$\gamma_1 = \sqrt{\dot{x}^2 + \dot{y}^2}, \quad \gamma_2 = -\arctan\frac{\ddot{x}}{\ddot{y}}. \quad (16)$$

This choice has a singularity when $\gamma_2 = \theta$ or $d = 0$, where the acceleration is ill-defined.

b) Choice 2.: To avoid the singularity at $d = 0$, define γ_2 as the acceleration component along the body-fixed y -axis:

$$\gamma_1 = \sqrt{\dot{x}^2 + \dot{y}^2}, \quad \gamma_2 = \ddot{y} \cos(\theta) - \ddot{x} \sin(\theta). \quad (17)$$

This choice avoids singularities except when $\gamma_1 = 0$, which corresponds to the system being at rest.

In both cases, the corresponding feedback control law is derived by defining ν as a stabilizing feedback law for the linear Brunovsky form system. A typical choice uses third-order error dynamics:

$$\begin{aligned}\nu_x &= \ddot{x}_d + K_2(\ddot{x}_d - \ddot{x}) + K_1(\dot{x}_d - \dot{x}) + K_0(x_d - x), \\ \nu_y &= \ddot{y}_d + K_2(\ddot{y}_d - \ddot{y}) + K_1(\dot{y}_d - \dot{y}) + K_0(y_d - y).\end{aligned}\quad (18)$$

The gains K_0 , K_1 , and K_2 are chosen such that the closed-loop dynamics are asymptotically stable, for instance using LQR design. The LQR cost function is:

$$J = \int_0^{\infty} (\mathbf{x}^\top \mathbf{Q} \mathbf{x} + \mathbf{u}^\top \mathbf{R} \mathbf{u}) dt. \quad (19)$$

The optimal \mathbf{K} is then computed via the solution to the Algebraic Riccati Equation.

This approach yields a structured and globally stable controller as long as the auxiliary variable singularities are avoided.

V. SIMULATION AND EXPERIMENTAL VALIDATION

We validate the proposed control strategies through a combination of simulation studies and real-world experiments conducted on a planar manipulation platform. The physical setup consists of a finger-like robotic pusher, paired with a vision-based state estimation using markers. The platform is designed to emulate the simplified kinematic model assumed in our derivations, but naturally introduces unmodeled effects such as surface friction variability, sensor latency, and mechanical compliance. Two representative tasks were selected for evaluation: static point and dynamic trajectory tracking. In both scenarios, the controller must ensure stable convergence of the pusher-slider system to the reference, despite disturbances and estimation noise.

Fig. 3 shows the comparison between simulated and experimental results for both tasks. Fig. 3a and Fig. 3b depicting the behavior for static point stabilization, where the goal is to control the slider to a fixed target location. Fig. 3c and 3d illustrate the performance for a dynamic trajectory tracking task, where the slider is commanded to follow a smooth, time-varying reference path.

The experimental results demonstrate strong agreement with simulation, highlighting the robustness and practical viability of the flatness-based control designs. Both the cascaded feedback and dynamic feedback linearization strategies successfully compensate for real-world imperfections, offering smooth, repeatable convergence to the reference despite limited model knowledge and sensor noise. This confirms the controllers' potential for real-time implementation in more complex manipulation and robotic pushing scenarios.

Making a direct comparison between the two control strategies is hard, since we are not yet working with optimally tuned control gains. However, at first sight we observe that the dynamic feedback linearization with the second choice of auxiliary state performs slightly better than the other two strategies, especially the first choice. This is likely due to the fact that the second choice of auxiliary state avoids the singularity at $d = 0$, which is a common occurrence in

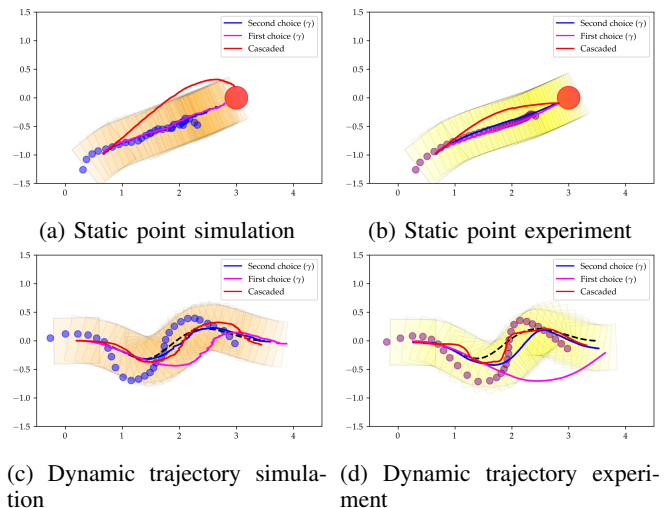


Fig. 3: Comparison of simulation and experimental results for the static point (top) and dynamic trajectory (bottom) tracking tasks. The left column shows simulation results, while the right column presents experimental results. All three methods are shown with a full line, while the reference trajectory for the latter is shown with a black dotted line.

practice. The first choice of auxiliary state, on the other hand, can lead to numerical issues when the system is close to this singularity.

VI. CONCLUSION AND OUTLOOK

Our study shows that simple, structured models like the slider-pusher system can provide a solid foundation for designing feedback controllers that perform reliably in real-world manipulation tasks. Despite the complexity of contact-rich dynamics, these models capture the essential behavior well enough to enable stable and effective closed-loop control, even in the presence of disturbances, model mismatches, and sensing imperfections.

Through both simulation and hardware experiments, we demonstrated that feedback strategies rooted in basic geometric and kinematic insights — rather than high-fidelity modeling or data-intensive learning — can deliver strong performance for tasks involving physical interaction. This highlights the enduring relevance of model-driven control, especially as a complementary component in systems that may eventually integrate learned policies or adaptive modules.

In a broader context, our results encourage revisiting and refining simple, interpretable models as a practical design tool for robust robot manipulation, particularly in scenarios where safety, stability, and real-time execution remain critical.

REFERENCES

- [1] M. T. Mason, “Mechanics and planning of manipulator pushing operations,” *The International Journal of Robotics Research*, vol. 5, no. 3, pp. 53–71, 1986.

- [2] S. Goyal, A. Ruina, and J. Papadopoulos, "Planar sliding with dry friction part 1. limit surface and moment function," *Wear*, vol. 143, no. 2, pp. 307–330, 1991.
- [3] —, "Planar sliding with dry friction part 2. dynamics of motion," *Wear*, vol. 143, no. 2, pp. 331–352, 1991.
- [4] G. Ziyang, A. Elibol, and N. Y. Chong, "Planar pushing of unknown objects using a large-scale simulation dataset and few-shot learning," in *2021 IEEE 17th International Conference on Automation Science and Engineering (CASE)*. IEEE, 2021, pp. 341–347.
- [5] K.-T. Yu, M. Bauza, N. Fazeli, and A. Rodriguez, "More than a million ways to be pushed. a high-fidelity experimental dataset of planar pushing," in *2016 IEEE/RSJ international conference on intelligent robots and systems (IROS)*. IEEE, 2016, pp. 30–37.
- [6] M. Bauza and A. Rodriguez, "A probabilistic data-driven model for planar pushing," in *2017 IEEE International Conference on Robotics and Automation (ICRA)*. IEEE, 2017, pp. 3008–3015.
- [7] F. R. Hogan and A. Rodriguez, "Feedback control of the pusher-slider system: A study of hybrid and underactuated contact dynamics," in *Algorithmic Foundations of Robotics XII*. Springer, 2020, pp. 800–815.
- [8] K. M. Lynch, H. Maekawa, and K. Tanie, "Manipulation and active sensing by pushing using tactile feedback," in *IROS*, vol. 1, 1992, pp. 416–421.
- [9] J. Zhou, M. T. Mason, R. Paolini, and D. Bagnell, "A convex polynomial model for planar sliding mechanics: theory, application, and experimental validation," *The International Journal of Robotics Research*, vol. 37, no. 2-3, pp. 249–265, 2018.
- [10] M. M. Ghazaei Ardakani, J. Bimbo, and D. Prattichizzo, "Quasi-static analysis of planar sliding using friction patches," *The International Journal of Robotics Research*, vol. 39, no. 14, pp. 1775–1795, 2020.
- [11] M. Fliess, J. Lévine, P. Martin, and P. Rouchon, "Flatness and defect of non-linear systems: introductory theory and examples," *International journal of control*, vol. 61, no. 6, pp. 1327–1361, 1995.
- [12] G. G. Rigatos, "Differential flatness theory and flatness-based control," in *Nonlinear Control and Filtering Using Differential Flatness Approaches*. Springer, 2015, pp. 47–101.
- [13] M. van Nieuwstadt, M. Rathinam, and R. Murray, "Differential flatness and absolute equivalence," in *Proceedings of 1994 33rd IEEE Conference on Decision and Control*, vol. 1, 1994, pp. 326–332 vol.1.
- [14] J. Lévine, "On the equivalence between differential flatness and dynamic feedback linearizability," *IFAC Proceedings Volumes*, vol. 40, no. 20, pp. 338–343, 2007, 3rd IFAC Symposium on System Structure and Control. [Online]. Available: <https://www.sciencedirect.com/science/article/pii/S1474667015366052>
- [15] J. Lévine, "On necessary and sufficient conditions for differential flatness," *Applicable Algebra in Engineering, Communication and Computing*, vol. 22, no. 1, pp. 47–90, 2011.
- [16] T. Lefebvre, S. De Witte, T. Neve, and G. Crevecoeur, "Differential flatness of slider–pusher systems for constrained time optimal collision free path planning," *Journal of Dynamic Systems, Measurement, and Control*, vol. 145, no. 6, p. 061001, 2023.
- [17] J. Diwold, B. Kolar, and M. Schöberl, "A trajectory-based approach to discrete-time flatness," *IEEE Control Systems Letters*, vol. 6, pp. 289–294, 2021.
- [18] F. Stoican, I. Prodan, and D. Popescu, "Flat trajectory generation for way-points relaxations and obstacle avoidance," in *2015 23rd Mediterranean Conference on Control and Automation (MED)*. IEEE, 2015, pp. 695–700.
- [19] F. Stoical, V.-M. Ivănușcă, I. Prodan, and D. Popescu, "Obstacle avoidance via b-spline parametrizations of flat trajectories," in *2016 24th Mediterranean Conference on Control and Automation (MED)*. IEEE, 2016, pp. 1002–1007.
- [20] F. Stoican, I. Prodan, D. Popescu, and L. Ichim, "Constrained trajectory generation for uav systems using a b-spline parametrization," in *2017 25th Mediterranean Conference on Control and Automation (MED)*. IEEE, 2017, pp. 613–618.
- [21] M. Greeff and A. P. Schoellig, "Flatness-based model predictive control for quadrotor trajectory tracking," in *2018 IEEE/RSJ International Conference on Intelligent Robots and Systems (IROS)*. IEEE, 2018, pp. 6740–6745.
- [22] S. Helling, M. Lutz, and T. Meurer, "Flatness-based mpc for underactuated surface vessels in confined areas," *IFAC-PapersOnLine*, vol. 53, no. 2, pp. 14 686–14 691, 2020.
- [23] M. Faessler, A. Franchi, and D. Scaramuzza, "Differential flatness of quadrotor dynamics subject to rotor drag for accurate tracking of high-speed trajectories," *IEEE Robotics and Automation Letters*, vol. 3, no. 2, pp. 620–626, 2017.
- [24] C. Aguilar-Ibáñez, H. Sira-Ramírez, M. S. Suárez-Castañón, E. Martínez-Navarro, and M. A. Moreno-Armendariz, "The trajectory tracking problem for an unmanned four-rotor system: flatness-based approach," *International Journal of Control*, vol. 85, no. 1, pp. 69–77, 2012.
- [25] D. R. Agrawal, H. Parwana, R. K. Cosner, U. Rosolia, A. D. Ames, and D. Panagou, "A constructive method for designing safe multi-rate controllers for differentially-flat systems," *IEEE Control Systems Letters*, vol. 6, pp. 2138–2143, 2021.
- [26] M. Greeff and A. P. Schoellig, "Exploiting differential flatness for robust learning-based tracking control using gaussian processes," *IEEE Control Systems Letters*, vol. 5, no. 4, pp. 1121–1126, 2020.
- [27] J. Rudolph, *Flatness-based control: An introduction*. Shaker Verlag, 2021.
- [28] E. Delaleau and J. Rudolph, "Control of flat systems by quasi-static feedback of generalized states," *International Journal of Control*, vol. 71, no. 5, pp. 745–765, 1998.
- [29] V. Hagenmeyer and E. Delaleau, "Exact feedforward linearization based on differential flatness," *International Journal of Control*, vol. 76, no. 6, pp. 537–556, 2003.
- [30] De Witte, Sander and Neve, Thomas and Lefebvre, Tom and Crevecoeur, Guillaume, "Reactive planning MPC of pusher-sliders with obstacle avoidance and imposed velocity profiles," in *2024 10th International Conference on Control, Decision and Information Technologies (CoDIT)*. IEEE, 2024, pp. 1469–1474. [Online]. Available: <http://doi.org/10.1109/codit62066.2024.10708389>
- [31] Neve, Thomas and De Witte, Sander and Lefebvre, Tom and Crevecoeur, Guillaume, "Trajectory planning of slider-pushers in cluttered environments with automatic switching," in *2024 European Control Conference (ECC)*. IEEE, 2024, pp. 2342–2349. [Online]. Available: <http://doi.org/10.23919/ecc64448.2024.10590891>
- [32] H.-G. Lee, *Dynamic Feedback Linearization*. Singapore: Springer Nature Singapore, 2022, pp. 227–261. [Online]. Available: https://doi.org/10.1007/978-981-19-3643-2_6